Long-term loading and recovery of a laminated glass slab with three different interlayers

Xavier Centelles[1], Fernández Pelayo[2], Manuel Aenlle López[2], J. Ramon Castro[1], Luisa F. Cabeza[1,*]

[1] GREiA Research Group, University of Lleida, Pere de Cabrera s/n, 25001, Lleida, Spain
[2] Department of Construction and Manufacturing Engineering, University of Oviedo, Campus de Gijón, Zona Oeste, Edificio 7, 33203, Gijón, Spain
*Corresponding author: Tel: +34 973003576. Email: luisaf.cabeza@udl.cat

Abstract

The mechanical behaviour of laminated glass plates and beams is affected in different ways by the shear stiffness of interlayer materials. Polymeric interlayers are viscoelastic materials, and therefore experience creep when subjected to long-term loading. In this paper, three laminated glass panels, each with a different interlayer material (PVB Clear, PVB ES, and SentryGlas), were placed between two laminated glass beams. A uniformly distributed load was applied during four months to study the effect of creep, and then was removed to see the deflection recovery during one month. The midspan vertical displacement of the two laminated glass beams remained almost constant over time, with a small variation that was attributed to the rubber sheets placed in the supports. The plate with SentryGlas had the lowest elastic deformation, creep, and residual deformation. The plate with PVB Clear had the highest elastic and total deformation. The plate with PVB ES had a similar initial deflection as SentryGlas, but was the one that experienced the highest creep. At the end of the test the plates still had a small residual deflection, which could be due to an incomplete deflection recovery. The flexural behaviour of the three laminated glass plates was simulated using a Finite Element Model, representing the loading, the creep, the unloading, and the deflection recovery stages.

Keywords

Laminated glass slab; long-term loading; deflection recovery; viscoelastic material; creep

1. Introduction

Laminated glass is obtained by bonding two or more glass layers with films of polymeric interlayer. The interlayer material transfers shear stresses between confronted glass surfaces [1,

2], and prevents glass shards from scattering in case of accidental breakage [3]. In terms of mechanical behaviour, glass is brittle and linear elastic, whereas polymeric interlayers are more ductile and viscoelastic, which means that their stiffness depends the loading history [4] and the working temperature [5,6,7].

With the aim of characterizing the viscoelastic behaviour of PVB, which is the most commonly used interlayer material for laminated glass, Pelayo et al. [5] performed dynamic tests on PVB films using a DMA equipment, but in more recent research [8] they identified that the high temperature and pressure during the autoclave process, together with the chemical transformations in the bond region, may affect the mechanical properties of the interlayer. That is why Andreozzi et al. [9] performed dynamic tests on PVB, but using laminated glass specimens instead of the polymeric film alone. In that sense, Ranocchiai et al. [10] performed an extensive review of the experimental techniques to evaluate the viscoelastic properties of the interlayer in laminated glass. They stated that the interlayers should be adhered to glass when tested.

More recently, Biolzi et al. [11] studied the viscoelastic response of double-lap joints under shear loading by performing relaxation and creep tests with three different interlayer materials: SentryGlas, PVB and plasticised PVB. The authors highlighted that the contribution of the interlayer material in laminated glass should be studied with laminated glass specimens, because the mechanical properties of the interlayer material not adhered to glass are not useful to predict the behaviour of laminated glass elements.

The long-term behaviour of viscoelastic materials can be predicted by doing tests of a shorter duration at different temperatures, and then applying the time-temperature superposition (TTS) to extrapolate the results to time values outside the tested range. The TTS principle states that the effect of increasing the time of loading is equivalent, in terms of mechanical behaviour, to the effect of increasing the working temperature [12]. The final mastercurve of the material is obtained applying a TTS model to the experimental short-time curves at different temperatures [13]. The relaxation master curve of a viscoelastic material can be expressed as a mathematical expression by means, i.e., of a Prony series (Eq. 1), where e_i and τ_i are the Prony coefficients. Some simulation programs use these coefficients in order to properly characterize the viscoelastic behaviour of the material.

$$E(t) = E_0 \left[1 - \sum_{i=1}^{n} e_i \left(1 - \exp\left(-\frac{t}{\tau_i}\right)\right)\right] \qquad \text{(Eq. 1)}$$

Laminated glass elements can be divided in two main groups, depending on the direction of the loading with respect to the placement of the layers: plates, when the load is perpendicular to the layers (e.g., facades, roofs or floors), or beams, when the glass layers are coplanar with the load. The mechanical performance of laminated glass plates is affected by the shear response of the interlayer [14]. Interfaces that are able to transfer bond stresses can contribute to increase the stiffness and strength of the composite material [15]. As a consequence, since the interlayer material is viscoelastic and affects the cohesiveness of laminated glass, the mechanical behaviour of laminated glass plates is also time- and temperature-dependant [16]. On the other hand, the contribution of the interlayer is negligible in the serviceability state of laminated glass beams [17], except in terms of lateral stability [18], but it affects the post-breakage behaviour and the glass breakage mode [17].

There are other types of loading for composite materials. Glass fibre reinforced polymer (GFRP) pipes may experience creep due to the effect of internal pressure and dead weight of the transported fluid [19-23]. Oil, gas, and water piping systems represent a big portion of the consumption of composites in industrial and civil engineering. They are required to remain operating during 50 years, and therefore they require long-term hydrostatic tests. GFRP pipes are lighter, cheaper, and easier to manufacture and install than metallic (e.g., copper) pipes, but they are also more prone to experience creep, especially when transporting fluids at high temperatures.

Figure 1 shows the typical mechanical response of a viscoelastic material [24]. When a constant stress (σ_1) is applied on a viscoelastic material, it presents an instantaneous strain associated with the elastic component ($\varepsilon_{1,e}$), and an additional strain growth over time, known as creep, due to the viscous component ($\varepsilon_{1,v}$). When the stress is removed, the material experiences a partial instantaneous recovery of the strain due to the elastic component ($\varepsilon_{r,e}$), and an additional progressive recovery over time due to the viscous component ($\varepsilon_{r,v}$). There may also be a residual deformation at the end due to plastic deformation (ε_p) or incomplete deflection recovery.

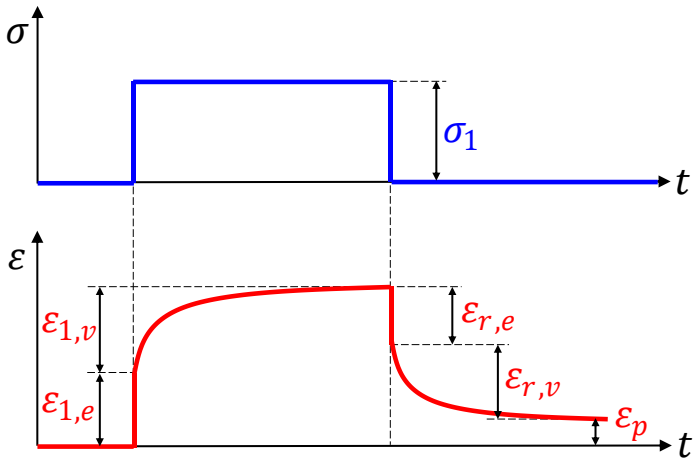

Figure 1. Creep compliance and recovery curves of a viscoelastic-plastic material.

This paper aims to identify all the stages presented in Figure 1 by applying a long-term distributed load on a laminated glass slab. To do so, three laminated glass plates, each with a different interlayer material (PVB Clear, PVB ES, and SentryGlas), were tested simultaneously in order to perform a comparative study between them. In addition to that, the beams that hold the laminated glass plates were also made of laminated glass. The goal was to compare the short- and long-term deformational response of vertically placed laminated glass beams with horizontally placed laminated glass plates. The load was applied during four months, then the load was removed and the slab remained unloaded for another month in order to study the deflection recovery and the residual deformation.

Very limited studies have been performed in the field of long-term creep analysis of laminated glass structures under bending. Valarinho et al. [25] performed flexural creep tests during 350 hours on laminated glass plates. They tested two laminated glass plates, each with a different interlayer material and number of glass layers: 3-layer PVB and 4-layer SentryGlas. They applied predictive models to extrapolate the measured creep to long-term (50 years) deflection. Significant differences were observed between the predictions based on viscoelastic models derived from Dynamic Mechanical Analysis (DMA) and the predictions based on the Findley power law, especially in the case of the PVB laminated glass panel, which experienced a much higher creep. One of the issues that the authors identified was that the duration of the flexural creep test was too limited, and future experiments should require longer creep periods.

This paper presents a longer creep period of over 3,000 hours. In addition to that, it compares laminated glass plates with three different interlayer materials (PVB Clear, PVB ES, and SentryGlas) instead of two. Another innovative aspect is that most creep tests found in the

literature, including the one presented by Valarinho et al. [25], finish before unloading the slab, while in this paper the recovery stage can also be evaluated.

The contribution of the interlayer material in the pre-breakage stage of laminated glass beams with vertical layers is negligible [26]. By contrast, it is an important factor for the lateral stability [27] and failure mechanisms [28]. Biolzi et al. [29] studied the post-breakage strength of laminated glass with DG41 (plasticised PVB) under long-term loading. The authors identified that the stiffness of the interlayer delayed the formation of cracks. In addition to that, in broken laminated glass beams under long-term loading, the cracks size and density increased over time due to the stress relaxation of the interlayer.

Since this paper focuses on the pre-breakage long-term behaviour of a laminated glass slab, the beams tested in this paper were oversized to prevent breakage and laterally constrained to prevent buckling. This means that the interlayer material of the laminated glass beams should not experience high stresses or creep during the test.

The flexural behaviour of the three different laminated glass plates was simulated using a numerical model implemented in ABAQUS. The main goal of that part was to study the similarities and differences between the experimental results and the simulation. Pelayo et al. [5] developed an ABAQUS numerical model to predict the long-term flexural behaviour of laminated glass plates under bending, with errors below 2% with respect to experimental tests.

Paolo Foraboschi [30] developed a model to study the out-of-plane flexural behaviour of composite laminates with elastoplastic interlayers. The model took into consideration the effect of interlayer material softening caused by creep, stress relaxation or plastic deformation. The resulting model could be applied to several composite materials, including laminated glass. The author highlighted that the nonlinearity of the interlayer plays a key role in the flexural behaviour of the composite element that should not be ignored.

2. Materials

The tested laminated glass slab is presented in Figure 2. The slab was composed of three laminated glass plates placed side by side, supported at two edges on two laminated glass beams. A rubber strip of thickness 5 mm was placed between glass plates and glass beams in order to prevent direct glass-to-glass contact. Rubber was also placed between the laminated glass beams and the wooden supports at both ends. The rubber strip was made from a combination of natural rubber (NR) with styrene-butadiene rubber (SBR), commercialized for general industrial applications. Each

wooden support was placed on top of a metallic beam (HEB 120), which in turn was placed on a high resistance metallic bench, with four wooden blocks to transfer the load to the floor.

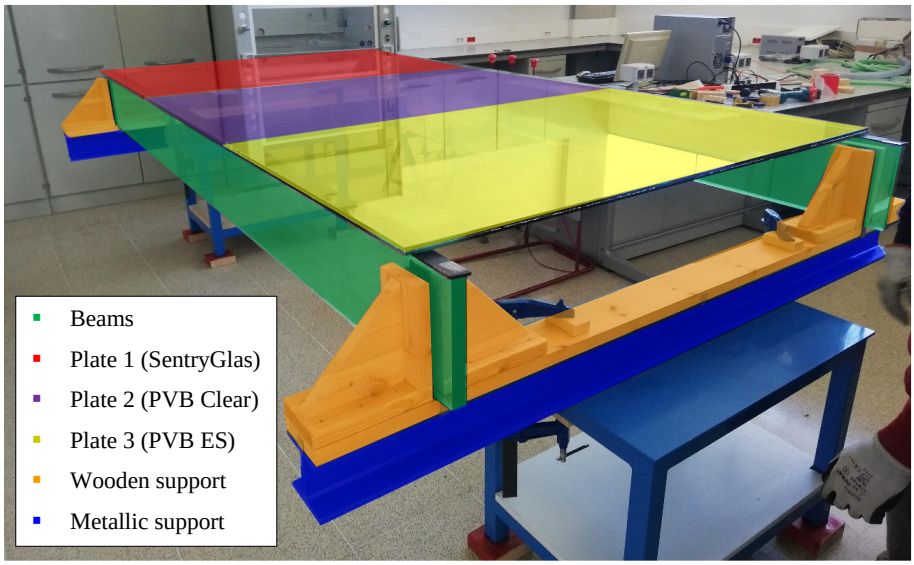

Figure 2. View of the laminated glass slab, where each component is highlighted in a different colour.

The laminated glass beams were composed of three tempered glass layers of length 3240 mm, height 250 mm, and thickness 10 mm. The Young modulus of the glass layers was 72 MPa, the Poisson ratio 0.22, and the density 2500 kg/m^3. The interlayer material of both laminated glass beams was 1.52 mm thick SentryGlas. The bending stiffness of glass is unaffected by the strengthening treatment [31].

Each of the three laminated glass plates had a size of 1580x1000 mm, with two layers of tempered glass, 8 mm thick each, and an interlayer of thickness 1.52 mm. Each plate had a different interlayer material: PVB Clear, PVB ES and SentryGlas. All interlayer materials were manufactured by Kuraray Europe GmbH, and the laminated glass elements were manufactured and supplied by CRISTEC Glass S.L. in Lleida (Spain).

PVB Clear is a polyvinyl butyral (PVB) with an enhanced transparency, but the mechanical properties of the standard PVB used in automobile windshields and glazing. The contribution of this interlayer in the serviceability limit state is usually considered negligible, especially for long-term loading and high temperatures [32].

PVB ES is a PVB with a lower level of plasticiser. Plasticisers increase the mobility of the polymer chains. By reducing the amount of plasticiser, the polymer becomes stiffer and its glass transition temperature increases [33].

SentryGlas is an ionomer that increased the resistance to impact and penetration of laminated glass, and for that reason it was originally used in hurricane glazing. Its application later expanded to structural elements [34], due to its good mechanical properties, and to laminated glass elements with metallic reinforcements [35,36] or embedded joints [37,38], because of its good adhesion to both glass and metals.

3. Methodology

3.1. Experimental set-up

The two laminated glass beams were initially placed on the wooden supports, and then the lateral restraints, also made of wood, were fixed with screws to the support (Figure 3 and

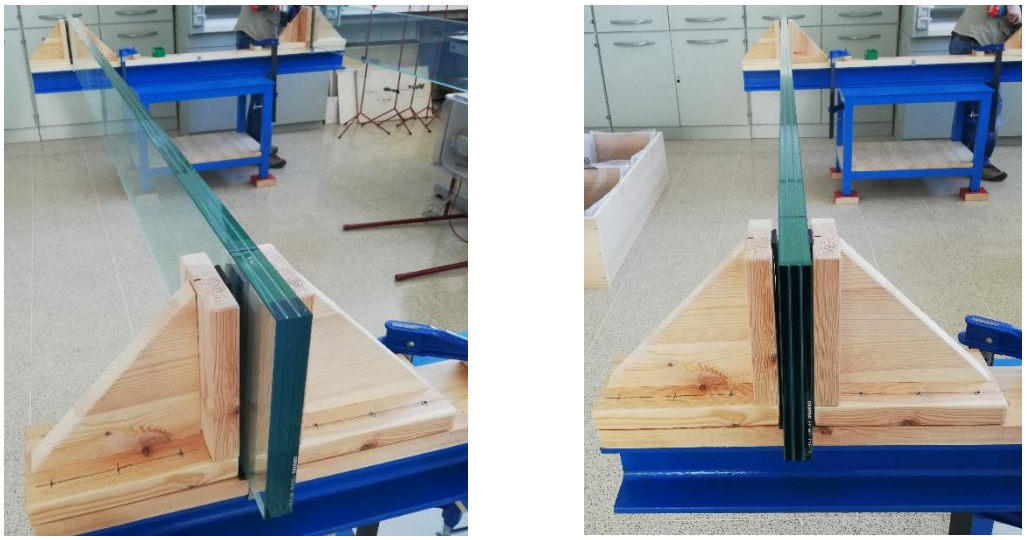

(a) (b)

Figure 4). Rubber layers were placed between glass and wood on all the contact surfaces. Then, the three different laminated glass plates were placed on top of the beams, also using an intermediate rubber layer in order to prevent direct glass-glass contact. The three plates were tested simultaneously in order to ensure that they were subjected to the same testing conditions (i.e., room temperature and humidity, load, time, etc.). A separation of 3 mm was kept between laminated glass plates in order to prevent undesirable interaction between plates that could affect the deflections and the readings of the displacement transducers (Figure 5).

Figure 3. Fastening of the wooden lateral restraints after the placement of the laminated glass beams.

(c)

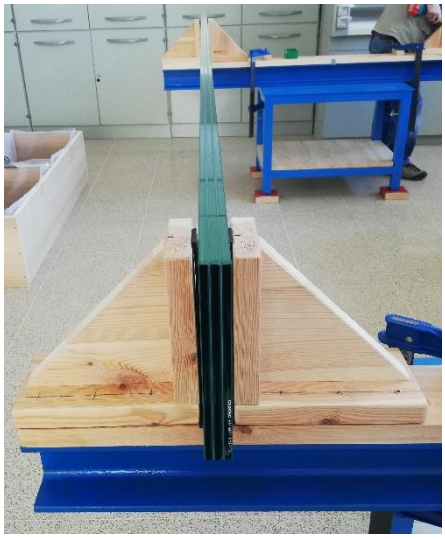

(d)

Figure 4. Beam placement on top of the wooden support with lateral restraints.

Figure 5. Separation between laminated glass plates.

The distance between the supports of the beams was 3 m. The separation between beams was 1.5 m. A sketch of the resulting laminated glass structure is presented in Figure 6 (lateral view), Figure 7 (front view), and Figure 8 (top view).

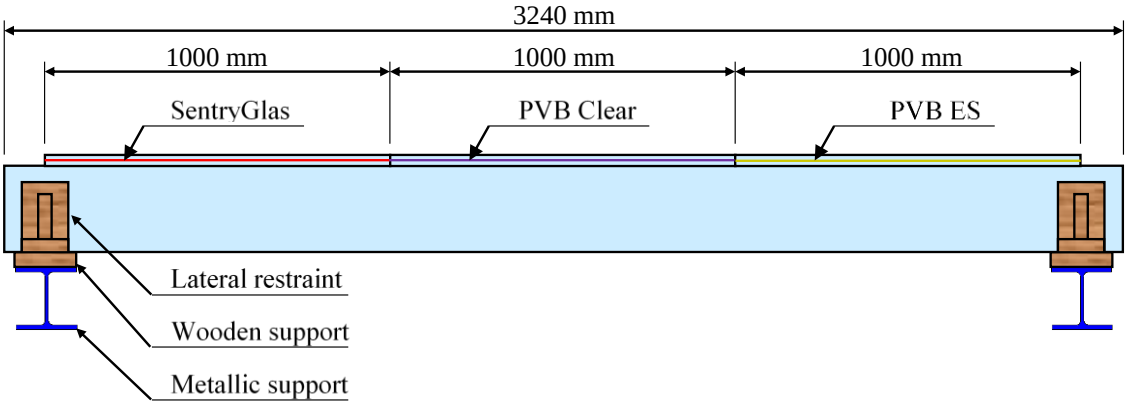

Figure 6. Lateral view of the laminated glass structure.

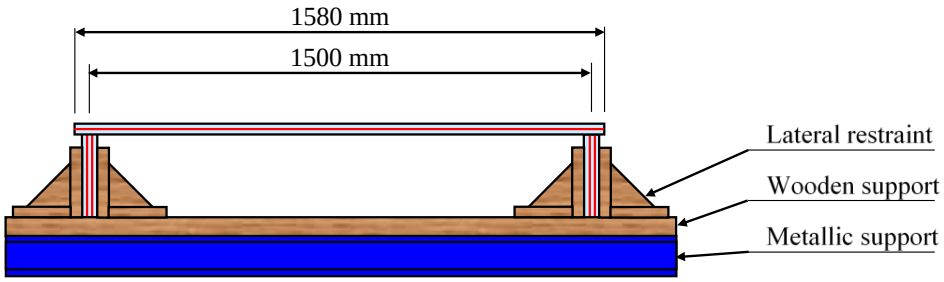

Figure 7. Front view of the laminated glass structure.

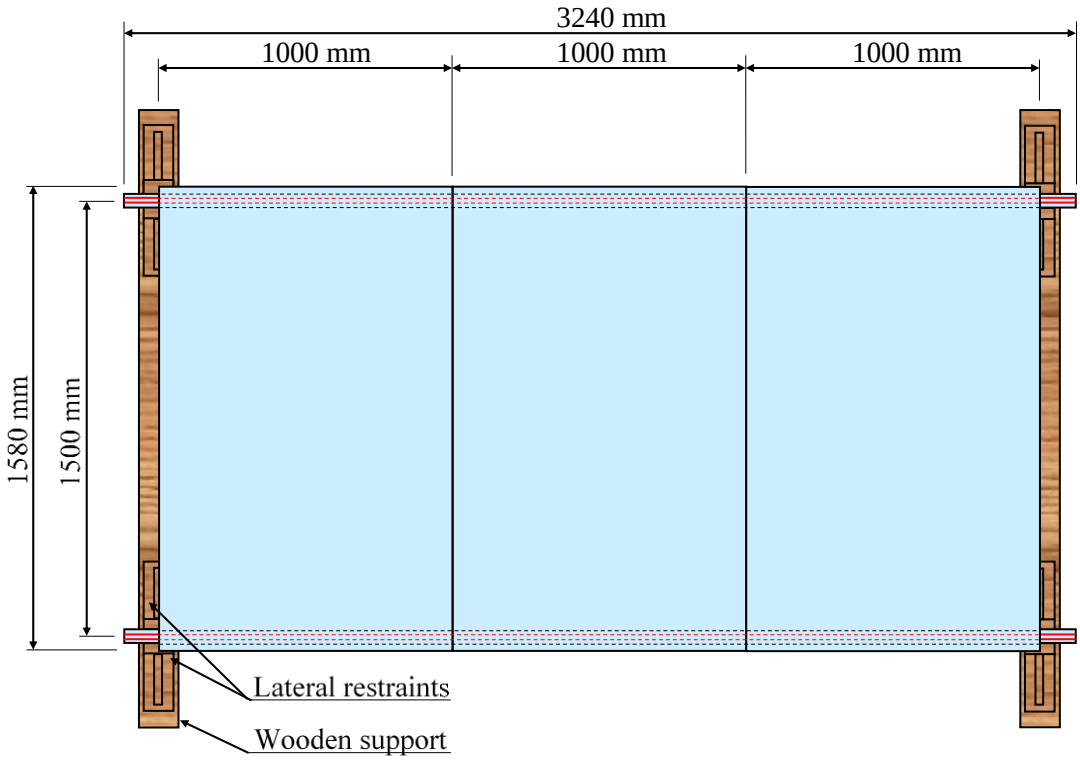

Figure 8. Top view of the laminated glass structure.

The tests were carried out in a laboratory at a controlled temperature of 23±1 ºC and relative humidity of 42±2 %. In order to measure the deflection of each of the three plates and two beams, five different displacement transducers (Novotechnik TR-0100) were placed at the bottom of the structure and connected to a data acquisition card (National Instruments NI-6212), which transferred the data to a computer using a LabVIEW program developed by the authors, with a sampling frequency of two measurements per minute (Figure 9). The displacement transducers were placed at the central point of the plates and the beams, where displacement was highest (Figure 10).

Figure 9. Arrangement of the displacement transducers.

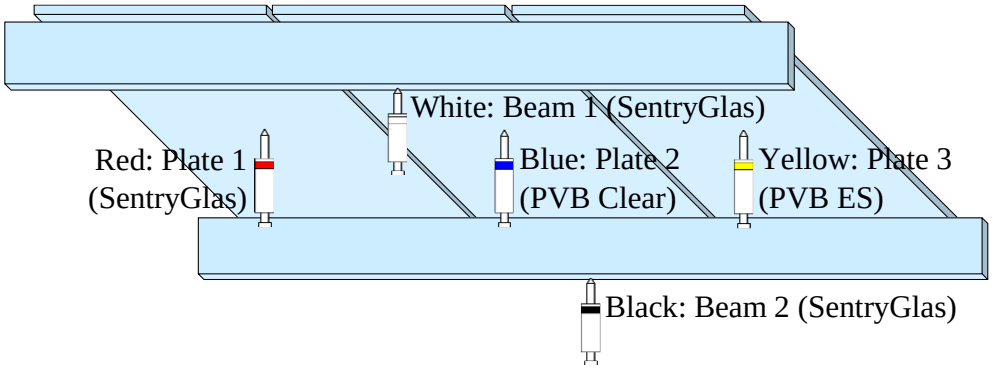

Figure 10. Sketch of the placement of the displacement transducers at the bottom of the laminated glass structure.

During experimentation, a homogeneous constant load of 3 kN/m^2 was applied, corresponding to the maximum load on floors of office areas (category B), or other public areas such as schools or restaurants (category C1) based on the standard EN 1991-1-1 [39]. The load was applied with water, in order to ensure a homogeneous surface distribution. In addition to that, using a transparent load on a transparent structure was considered to be more consistent from an aesthetical point of view. A wooden formwork with twelve compartments acted as retaining wall for the water (Figure 11). The load was applied by gradually pouring water buckets on each of the compartments of the formwork. First, a bucket was poured in each of the 12 compartments, and the process was repeated several times, until the desired load was reached. The loading operation took approximately two hours to complete. A polymeric film was placed between the water and the wooden frame in order to avoid leakage, and another film was placed top to prevent water evaporation (Figure 12). The constant load was maintained during four months, which is approximately the same one previously estimated by Andreozzi et al. [14] when defining the relaxation master curves of PVB. After four months the load was removed with the help of a hose connected to a vacuum pump. The unloading process took approximately half an hour to complete. After the unloading, the test lasted one additional month in order to study the recovery of the deformations and measure the residual deflection.

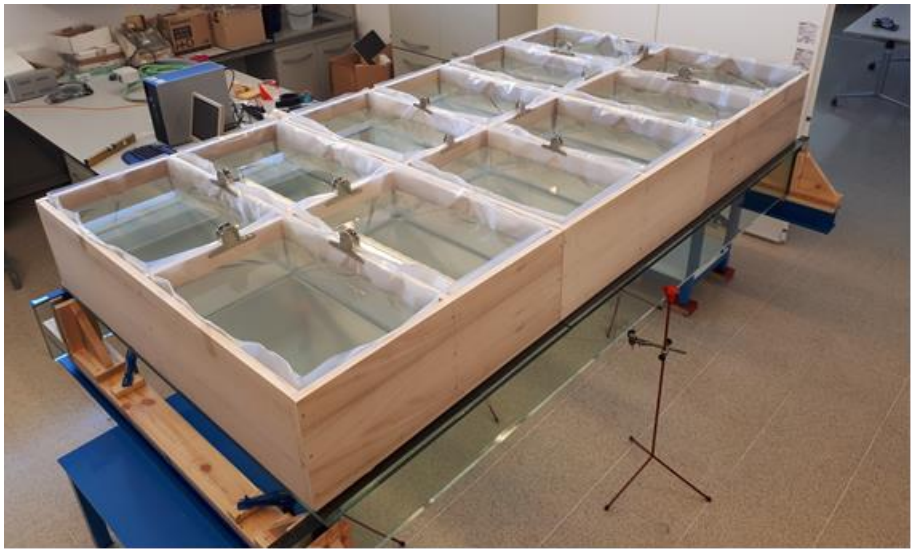

Figure 11. Laminated glass slab with the full load of water poured into the 12 compartments of the wooden formwork, with plastic bags to prevent water leakage.

Figure 12. Laminated glass slab loaded with water and covered with a polymeric film to prevent water evaporation.

3.2. Numerical model

The bending deflection of the laminated glass plates investigated in this paper was simulated using a finite element model (FEM) implemented in ABAQUS. In the FEM, 3D linear shell continuum elements (SC8R) were used for the glass layers whereas the PVB layer was meshed with 3D linear hexahedral elements (C3D8R). Each layer of the laminated glass is discretized with one element along its thickness whereas an approximate size of 30 mm was used for the other dimensions. This meshing technique has been demonstrated to be adequate to reproduce the laminated glass behaviour with a relatively low computational time [5, 40]. The mesh is presented in Figure 13.

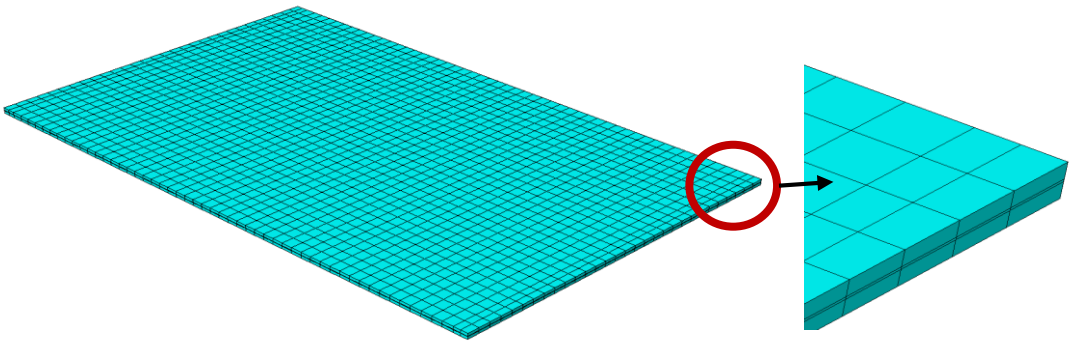

Figure 13. Finite element model for the plates.

In order to consider the effect of the rubber bands used in the experiments between glass plates and beams (see Figure 11 and Figure 12), a simply supported linear elastic boundary condition with stiffness 120 kN/m was assumed in the FEM simulations. This value was obtained considering a constant linear compression in the rubber strips using a material Young's modulus of 15 MPa [41, 44]. The load was modelled in four steps replicating the process followed in the experiments: first, linear loading until maximum pressure (3 kN/m^2), second, creep test, third, linear load removal until the pressure is removed (discharge), and fourth, relaxation test (recovery). The loading process is presented in Figure 14a. Self-weight load was also considered to the plate.

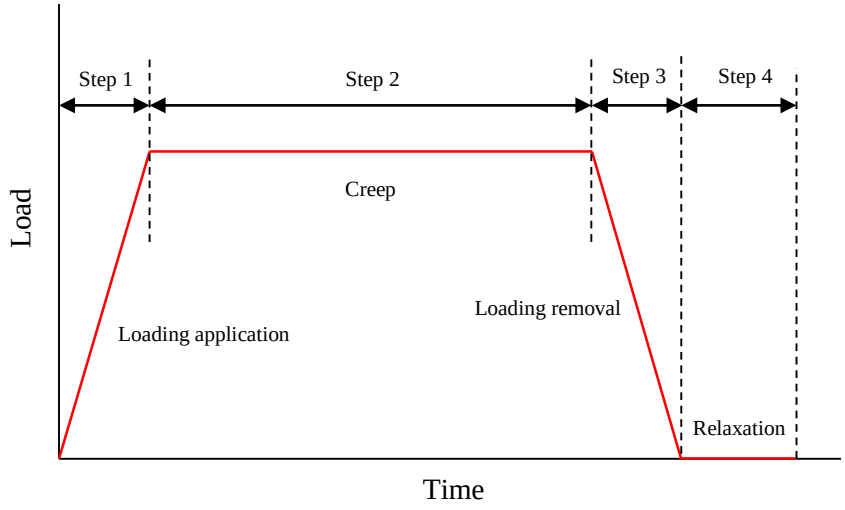

Figure 14a. Loading process using in the FEM simulations.

With respect to materials modelling, a linear elastic behaviour was considered for glass layers ($E = 72\ GPa, \nu = 0.23$) [5]. As regards the interlayers, a linear viscoelastic behaviour was assumed. The material model was implemented in ABAQUS using the Generalized Maxwell Model by means of Prony series equation (see Eq. (1)). The viscoelastic model coefficients were obtaining by fitting the master curves of the interlayers using MATLAB. Each material master curve was constructed using the TTS WLF model [5, 12] and the short time curves retrieved from manufacturer [41]. The shear master curves for each interlayer are presented in Figure 14. On the other hand, the Prony series coefficients fort each interlayer are presented in Table 14b for a reference temperature of 23^oC.

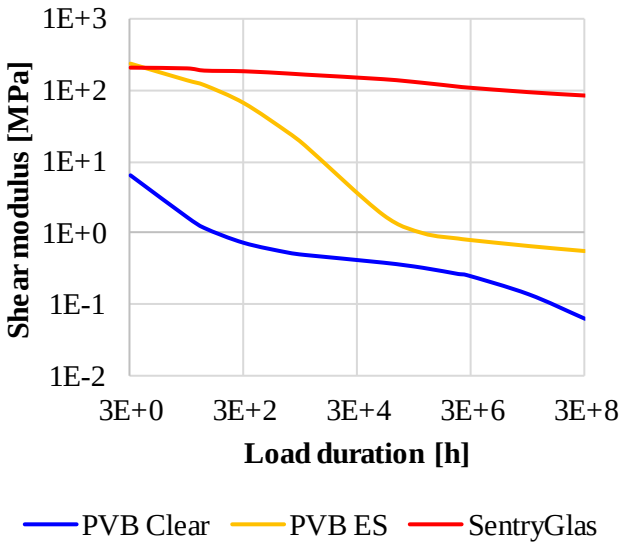

Figure 14. Shear modulus of the three tested interlayer materials as a function of load duration (from three seconds to ten years), at a temperature of 23 ºC, according to the manufacturer [41].

Table 14b. Prony coefficients (see Eq. (1)) for the interlayers

Sentry Glass		PVB ES		PVB Clear	
τ_i [s]	e_i	τ_i [s]	e_i	τ_i [s]	e_i
2.7978e-05	6.9639e-02	4.2529e-07	2.0743e-01	9.8967e-02	6.5673e-01
2.1308e-03	4.5248e-02	8.5814e-06	1.3132e-01	7.5342e-01	2.0077e-01
1.6228e-01	5.2259e-02	1.7315e-04	1.6307e-01	5.7357e+00	1.0927e-01
1.2360e+01	1.4778e-01	3.4938e-03	1.8233e-01	4.3665e+01	1.4716e-02
9.4131e+02	3.1893e-01	7.0496e-02	1.7227e-01	3.3242e+02	8.6423e-03
7.1690e+04	2.5120e-01	1.4224e+00	8.2456e-02	2.5307e+03	6.9512e-05
5.4600e+06	7.3016e-02	2.8701e+01	3.4552e-02	1.9266e+04	1.6249e-03
4.1583e+08	3.3058e-02	5.7912e+02	1.6069e-02	1.4667e+05	7.8093e-04
3.1670e+10	5.5461e-03	1.1685e+04	4.9452e-03	1.1165e+06	1.3491e-03
2.4120e+12	1.8182e-03	2.3578e+05	2.9544e-03	8.5001e+06	1.5284e-03
1.8370e+14	3.7681e-04	4.7575e+06	1.0820e-03	6.4710e+07	9.8863e-04
1.3990e+16	2.5896e-04	9.5994e+07	5.6822e-04	4.9263e+08	1.1571e-03
1.0655e+18	1.0658e-04	1.9369e+09	9.5460e-05	3.7503e+09	5.8693e-04

4. Results and discussion

4.1. Experimental results

The displacement values measured by the transducers placed on each plate corresponded to the sum of the displacements of the plate and the beam. In order to make a proper comparison between the three plates, as well as between experimental results and simulations, it was necessary to isolate the displacement of the plates (Figure 15). That is why the vertical displacement of the beams was subtracted from the measurements of the transducers on each plate. The displacement measured from the transducer placed under the beam was subtracted from the central plate, and half that value was subtracted from the lateral plates (Eq, 3 and 4).

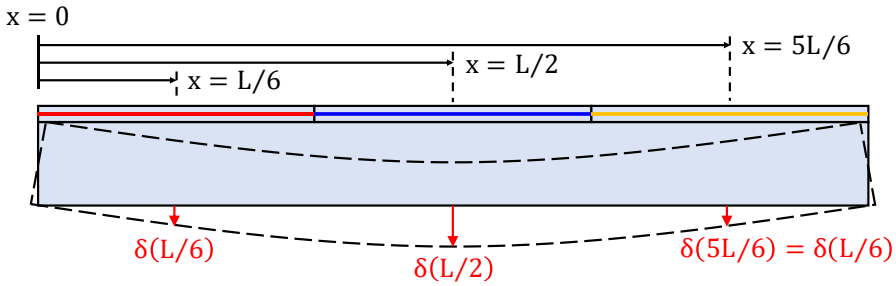

Figure 15. Vertical displacement of the beam at the points where the displacement transducers were placed on each plate.

$$\delta(x) = \frac{qx}{24EI}(x^3 - 2lx^2 + l^3) \quad \text{(Eq. 3)}$$

$$\frac{\delta(L/6)}{\delta(L/2)} = \frac{41}{81} \cong 0.5 \quad \text{(Eq. 4)}$$

Figure 16 shows the evolution of vertical displacement during the load application time, while Figure 17 shows the evolution of the vertical displacement during the unloading process. These figures indicate that the load application and removal were progressive and homogeneous over the whole surface of the slab. Since the loading process took over two hours to complete, the creep that may have happened during that initial stage could not be measured. What is indicated as creep hereinafter refers to the additional measured deflection starting from the end of the loading process. The same approach was adopted for the deflection recovery during the unlading process, which lasted approximately 30 minutes.

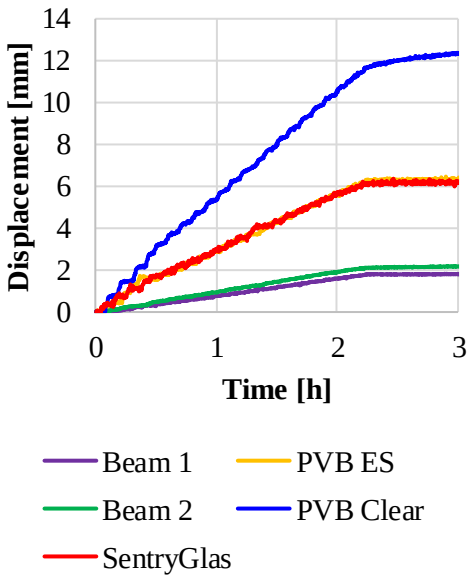

Figure 16. Measured vertical displacements during the loading process.

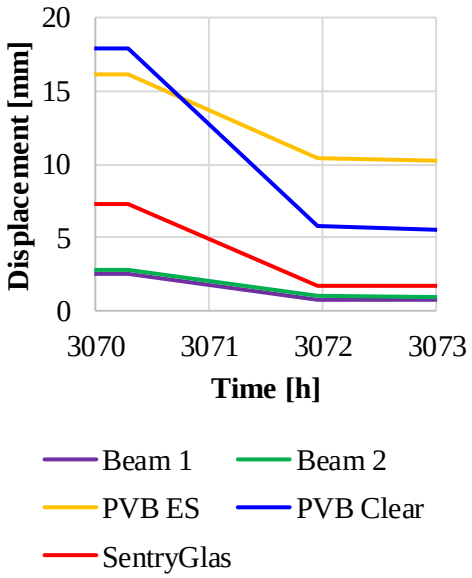

Figure 17. Measured vertical displacements during the unloading process.

Figure 18 presents the time evolution of the deflection for the three laminated glass plates and the two laminated glass beams. These results show that the initial vertical displacement of the laminated glass plates with PVB ES and SentryGlas was very similar, whereas the vertical displacement of the laminated glass plate with PVB Clear was almost the double. At the end of the four initial months, before unloading the slab, the vertical displacement of the plate with PVB ES was closer to the one with PVB Clear than the one with SentryGlas. The plate with PVB ES was the one that experienced the highest creep, and the one with SentryGlas, the lowest. The experimental results obtained by Valarinho et al. [25] also concluded that the creep deformation

was higher in the laminated glass panel with PVB than in the one with SentryGlas. After unloading the slab, there was a gradual recovery of the deflection, and the plate with SentryGlas had the lowest residual deflection.

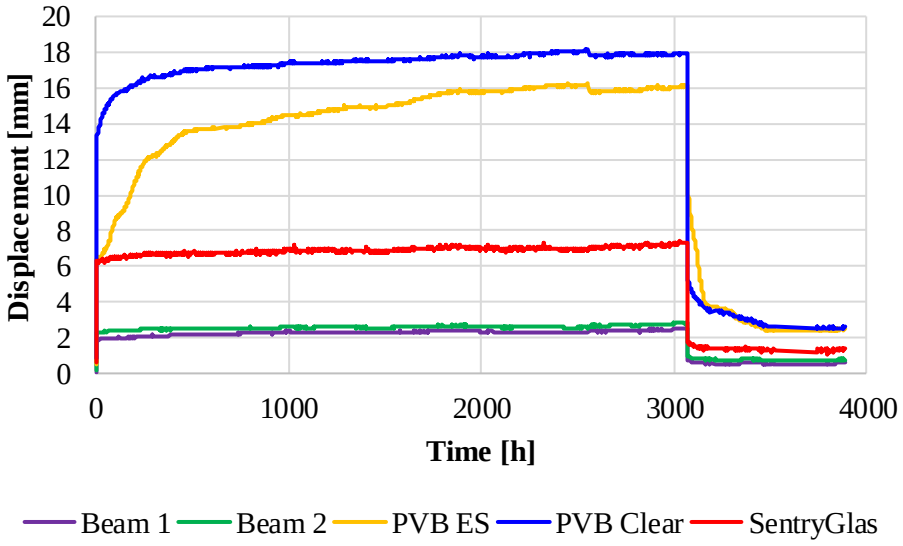

Figure 18. Vertical displacements during the whole test duration.

Table 1 shows an overview of the vertical displacement experienced by each load-bearing glass element in each of the stages. The elastic deflection corresponds to the vertical displacement experienced during the loading process, while viscous deflection refers to the displacements over time with a constant load. The same thing applies to the elastic and viscous recovery in the unloading process. The different vertical displacements presented there correspond to the ones previously mentioned in Figure 1. In all three plates, the elastic recovery almost matched the initial elastic deflection. The plate with PVB Clear experienced the highest elastic deflection and overall vertical displacement after four months. However, the plate with PVB ES was the one that experienced the highest creep, almost doubling the creep of the plate with PVB Clear, and multiplying ten-fold the creep of the plate with SentryGlas. At the end of the test, the two plates with PVB had the same residual deformation, which doubled the one of the plate with SentryGlas.

Table 1. Displacement measured on each beam and plate separating the elastic and the viscous components.

Component	**Elastic deflection**	**Viscous deflection**	**Elastic recovery**	**Viscous recovery**	**Residual deformation**
Beam 1	1.8 mm	0.5 mm	1.8 mm	0.2 mm	0.3 mm
Beam 2	2.2 mm	0.5 mm	2.2 mm	0.2 mm	0.3 mm
Plate 1 (SentryGlas)	6.3 mm	1.0 mm	5.6 mm	0.5 mm	1.2 mm

Plate 2 (PVB Clear)	13.0 mm	5.0 mm	13.0 mm	2.5 mm	2.5 mm
Plate 3 (PVB ES)	6.4 mm	9.7 mm	7.1 mm	6.8 mm	2.5 mm

The results show a small creep effect over time experienced by the laminated glass beams. According to the literature, the bending stiffness of laminated glass beams does not depend on the shear stiffness of the interlayer material in the pre-breakage stage [3,17]. This means that, if a laminated glass beam were to experience creep, it would be caused by glass. However, the creep experienced by glass under these testing conditions, in terms of load duration (four months) and temperature (23±1 ºC) should be negligible [30]. That is why it seems much more likely that this small viscous deflection and recovery, as well as the residual deflection, were caused by the rubber sheets placed below the beams. In fact, according to the manufacturer, the rubber combination of NR and SBR used for this test can experience a plastic deformation of 40% under compressive loading. Therefore, it is reasonable to consider that the rubber strips of thickness 5 mm experienced a 1 mm plastic deformation after the loading phase.

Figure 14 presents the relaxation master curve of the three interlayer materials, generated with data supplied by the manufacturer [29]. Comparing the results from the three laminated glass plates in Figure 18 with the results from the polymeric films in Figure 14, it is possible to see the correlation between the shear stiffness of the interlayer and the bending stiffness of the laminated glass plates [9,16]. With a lower shear stiffness of the interlayer, there was a higher vertical displacement of the laminated glass plate, as a consequence of the reduction of the bending stiffness. For short-duration loading, the shear stiffness of PVB ES and SentryGlas was very similar, whereas the shear stiffness of PVB Clear was much lower. During the first few hours of test, the plates with PVB ES and SentryGlas presented a similar vertical displacement and evolution over time. However, as time advanced, the vertical displacement of the plate with PVB ES increased at a higher rate, as a consequence of the progressive decrease of the interlayer stiffness.

Since the test was symmetrical and the two laminated beams were identical, their vertical displacement were very similar. In fact, the small differences may be due to inaccuracies during the calibrating process of the displacement transducers or the settling of the beams. The contribution of the interlayer in the serviceability state of laminated glass beams (vertical glass layers) is negligible. The shear stiffness of the interlayer material would affect the critical buckling moment of the laminated glass beams [43]. However, in this case, the lateral displacement of the laminated glass beams was restricted by the connection at the upper surface with the laminated glass plates and at both ends with the wooden supports. The measuring of displacements on the central point of the beams was almost constant over time, with a variation

of 0.5 mm after four months of loading. At the end of the test, after unloading the slab during one month, the remaining vertical displacement was of 0.3 mm. Such small creep and residual deflection may come from the rubber strips placed between glass and the wooden supports rather than from the glass elements, because the creep of glass at room temperature for the duration of this test should be unperceivable [42].

4.2. Simulation results

The displacements obtained with FE model (defined in Section 3.2) at the same points measured in the experiments are presented in Fig. 9. The results obtained in the numerical simulations, together with those measured in the experimental tests, are presented in Figure 19. A detailed comparison between the experimental and the predicted results are shown in Figure 20 for the first part of the test (approximately the first 4 hours).

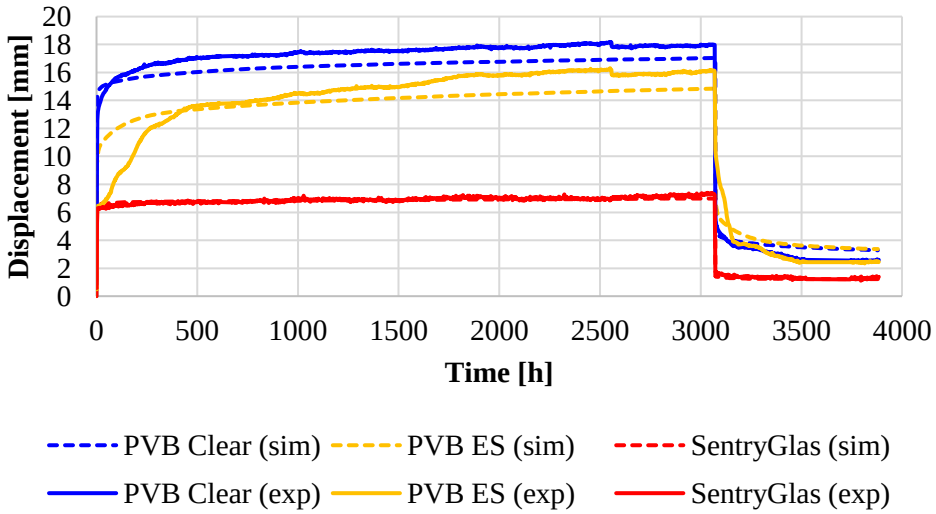

Figure 19. Experimental results and Analytical prediction (Eq. 1) for the three tested glass plates.

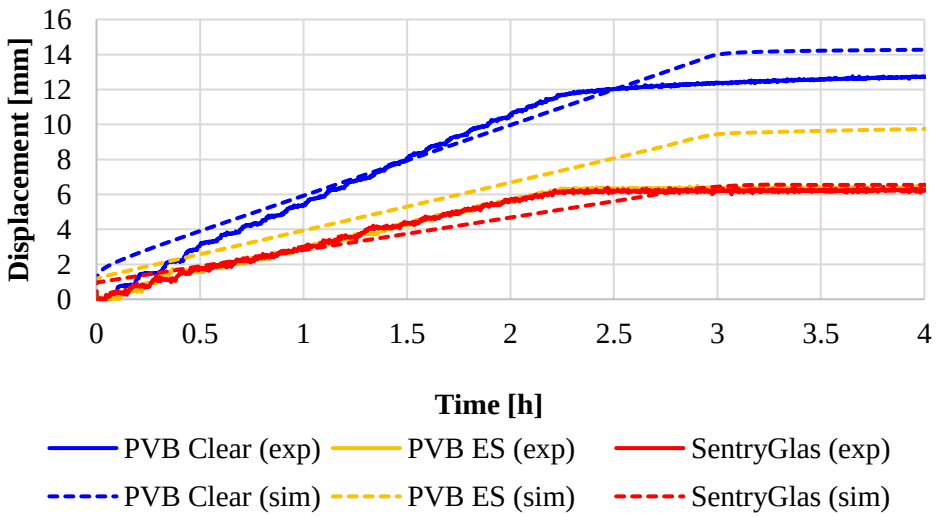

Figure 20. Detail of the loading and beginning of the creep test for the three different plates.

From the results it can be inferred that the response of the laminated glass plate with PVB Clear interlayer is predicted with an error less than 4.6% in the loading-creep process. However, the unloading is predicted with less accuracy, the maximum error being 32%.

With respect to the SentryGlas laminated glass plate, the response is predicted with an error less than 4.5% in the loading-creep steps, whereas the unloading is predicted with an error less than 10%.

Larger errors were encountered for the plate with PVB ES interlayer, the maximum errors being 25% in the loading process, 12% in the creep test and, 25% for the relaxation test. This plate presents an anomalous behaviour in the period from 0 to 400 hours (different to that exhibited by the PVB Clear and SentryGlas plates), which cannot be predicted with the FE model. This effect could be attributed to a material misbehaviour or to some problems in the experimental tests, but an explanation to this non-typical behaviour was not found.

Valarinho et al. [25] simulated the creep deformation of two laminated glass plates: one with SentryGlas and another with PVB. They compared the deflection prediction of their model with other results found in the literature, and bigger differences were found for the plate with PVB, probably because its creep deformation was significantly higher. This is in line with the results of this paper: the laminated glass plate with higher creep deformation was the one with larger errors in the simulation.

The simulation was carried out under the assumption that all three plates were placed horizontally. The beam deflection and its consequent in-plane angular variation may cause a tilt in the

supported plates. However, that tilt was considered to be negligible given the small angular variation experienced by the beams. In fact, the angle at the supports of the beams (φ) was of approximately 0.05º, as shown in Eq. 5.

$$\varphi(x=0) = \varphi(x=L) = \frac{qL^3}{24EI} \approx 0.05^o \quad \text{(Eq. 5)}$$

Finally, the maximum displacement in the plates for different time intervals were predicted with the FEM. The values are presented in Table 20a. Although some discrepancies have been encountered between the numerical and experimental results, the predictions can be used for comparison proposes as well as to illustrate the different long term creep behaviour of each interlayer.

Table 20a. Maximum deflection predicted with the FEM for different time periods.

Material	5 years [mm]	10 years [mm]	20 years [mm]	50 years [mm]
SentryGlass	7.745	7.937	8.275	8.982
PVB ES	17.41	17.89	18.11	18.26
PVB CLEAR	18.92	19.39	19.72	20.54

5. Conclusions

A long-term duration test was performed on a laminated glass slab. Three laminated glass layers, with a different interlayer each (PVB Clear, PVB ES, and SentryGlas), were placed on top of laminated glass beams. The separation between beams was of 1.5 m, and the span of the beams was 3 m. A homogeneous load of 3 kN/m^2 was placed on the slab during four months, and the displacement of each load-bearing element was measured over time. In order to evaluate the deflection recovery and the residual deflection, the measuring of the vertical displacement continued during one month after removing the load.

The two beams experienced almost no creep and no residual deflection. In fact, the creep and residual deformation measured in this case may be from the rubber strips placed between the laminated glass beams and the wooden supports, rather than from the laminated glass beams. The shear stiffness of the interlayer material did not have a significant influence in the serviceability limit state of laminated glass beams. However, according to literature, the interlayer material may have an important effect in the ultimate limit state of laminated glass beams [17], which was not studied in this paper, and in their lateral stability [18], which was restricted in this experiment by

the addition of the horizontally placed laminated glass plates at the top of the beams and the wooden lateral restraints at both ends of the beams.

The elastic recovery measured by each load-bearing element was very similar to its initial elastic displacement. The laminated glass plate with SentryGlas experienced the lowest value of elastic deflection, creep, and residual deflection. The laminated glass plate with PVB Clear experienced the highest elastic and total vertical displacement, but the plate with PVB ES experienced the highest creep.

The bending deflection of the laminated glass plates were predicted using a FEM. Although there are significant uncertainties in the mechanical properties of the interlayers, due to its viscoelastic nature, and the test developed in this paper was complex, the deflections can be predicted with a reasonable accuracy for the laminated glass plates with PVB Clear and SentryGlas interlayers. Larger errors were encountered in the plate with PVB ES in both loading-creep stage and unloading process. However, an anomalous behaviour was observed for this plate during the experiment, which does not follow the same tendency during the loading-creep process as the two other plates.

The fact that only one displacement transducer was used for each plate could be a possible source of inaccuracies in the experimental test. One or two additional transducers should have been placed on each glass plate near the edges in order to eliminate the possible inaccuracies caused by the deformation of the constraints: between beams and plates the rubber deforms under loading and is probably responsible for most of residual deformation.

Acknowledgements

The work was partially funded by CRISTEC with CDTI funds (IDI-20160588). The authors at the University of Lleida would like to thank the Catalan Government for the quality accreditation given to their research group GREiA (2017 SGR 1537). GREiA is certified agent TECNIO in the category of technology developers from the Government of Catalonia. This work is partially supported by ICREA under the ICREA Academia programme. The financing support given by the Spanish Ministry of Economy and Competitiveness through the project BIA2014-53774-R is gratefully appreciated. Xavier Centelles would like to thank University of Lleida for his research fellowship and to the University of Oviedo for hosting his secondment during 2019.

R. Rafiee, A. Ghorbanhosseini. Developing a micro-macromechanical approach for evaluating long-term creep in composite cylinders. Thin–Walled Structures 151 (2020) 106714. https://doi.org/10.1016/j.tws.2020.106714

R. Rafiee, A. Ghorbanhosseini. Analyzing the long-term creep behavior of composite pipes: Developing an alternative scenario of short-term multi-stage loading test. Composite Structures 254 (2020) 112868. https://doi.org/10.1016/j.compstruct.2020.112868

R. Rafiee, B. Mazhari. Simulation of the long-term hydrostatic tests on Glass Fiber Reinforced Plastic pipes. Composite Structures 136 (2016) 56-63. https://doi.org/10.1016/j.compstruct.2015.09.058

R. Rafiee, B. Mazhari. Evaluating long-term performance of Glass Fiber Reinforced Plastic pipes subjected to internal pressure. Construction and Building Materials 122 (2016) 694–701. http://dx.doi.org/10.1016/j.conbuildmat.2016.06.103

R. Rafiee, B. Mazhari. Modeling creep in polymeric composites: Developing a general integrated procedure. International JournalofMechanicalSciences99(2015)112–120. http://dx.doi.org/10.1016/j.ijmecsci.2015.05.011

References

1. L. Galuppi, G. Royer-Carfagni. Enhanced Effective Thickness of multi-layered laminated glass. Composites: Part B 64 (2014) 202–213. https://doi.org/10.1016/j.compositesb.2014.04.018
2. X. Centelles, J.R. Castro, L.F. Cabeza. Double-lap shear test on laminated glass specimens under diverse ageing conditions. Construction and Building Materials 249 (2020) 118784. https://doi.org/10.1016/j.conbuildmat.2020.118784
3. L. Galuppi, G. Royer-Carfagni. The post-breakage response of laminated heat-treated glass under in plane and out of plane loading. Composites Part B 147 (2018) 227–239. https://doi.org/10.1016/j.compositesb.2018.04.005
4. L. Galuppi, G. Royer-Carfagni. Laminated beams with viscoelastic interlayer. International Journal of Solids and Structures 49 (2012) 2637-2645. https://doi.org/10.1016/j.ijsolstr.2012.05.028
5. F. Pelayo, M.J. Lamela-Rey, M. Muniz-Calvente, M. López-Aenlle, A. Álvarez-Vázquez, A. Fernández-Canteli. Study of the time-temperature-dependent behaviour of PVB: Application to laminated glass elements. Thin-Walled Structures 119 (2017) 324–331. https://doi.org/10.1016/j.tws.2017.06.030
6. C. Suwen, C. Xing, W. Xiqiang. The mechanical behaviour of polyvinyl butyral at intermediate strain rates and different temperatures. Construction and Building Materials 182 (2018) 66–79. https://doi.org/10.1016/j.conbuildmat.2018.06.080

7. A. Rühl, S. Kolling, J. Schneider. Characterization and modeling of poly(methyl methacrylate) and thermoplastic polyurethane for the application in laminated setups. Mechanics of Materials 113 (2017) 102-111. https://doi.org/10.1016/j.mechmat.2017.07.018
8. M. López-Aenlle, A. Noriega, F. Pelayo. Mechanical characterization of polyvinil butyral from static and modal tests on laminated glass beams. Composites Part B 169 (2019) 9–18. https://doi.org/10.1016/j.compositesb.2019.03.077
9. L. Galuppi, G. Royer-Carfagni. Effective thickness of laminated glass beams: New expression via a variational approach. Engineering Structures, vol. 38, pp. 53–67, 2012. https://doi.org/10.1016/j.engstruct.2011.12.039
10. G. Ranocchiai, F. Zulli, L. Andreozzi, M. Fagone. Test methods for the determination of interlayer properties in laminated glass. Journal of Materials in Civil Engineering 29 (2017) 4016268. https://doi.org/10.1061/(ASCE)MT.1943-5533.0001802
11. L. Biolzi, S. Cattaneo, M. Orlando, L.R. Piscitelli, P. Spinelli. Constitutive relationships of different interlayer materials for laminated glass. Composite Structures 244 (2020) 112221. https://doi.org/10.1016/j.compstruct.2020.112221
12. M.L. Williams, R.F. Landel, J. Ferry. The temperature dependence of relaxation mechanisms in amorphous polymers and other glass-forming liquids. Journal of the American Chemical Society 77 (1955)3701-3707 https://doi.org/10.1021/ja01619a008
13. A. Álvarez-Vázquez, A. Ferández-Canteli, E. Castillo Ron, F. Pelayo, M. Muñiz-Calvente, M.J. Lamela Rey. A time- and temperature-dependent viscoelastic model based on the statistical compatibility condition. Materials & Design 193 (2020) 108228. https://doi.org/10.1016/j.matdes.2020.108828
14. L. Andreozzi, S.B. Bati, M. Fagone, G. Ranocchiai, F. Zulli. Dynamic torsion tests to characterize the thermo-viscoelastic properties of polymeric interlayers for laminated glass. Construction and Building Materials 65 (2014) 1–13. https://doi.org/10.1016/j.conbuildmat.2014.04.003
15. H.C. Biscaia. Closed-form solutions for modelling the response of adhesively bonded joints under thermal loading through exponential softening laws. Mechanics of Materials 148 (2020) 103527. https://doi.org/10.1016/j.mechmat.2020.103527
16. T. Serafinavičius, J.-P. Lebet, C. Louter, T. Lenkimas, A. Kuranovas. Long-term laminated glass four point bending test with PVB, EVA and SG interlayers at different temperatures. Procedia Engineering 57 (2013) 996–1004. https://doi.org/10.1016/j.proeng.2013.04.126
17. J. Belis, J. Depauw, D. Callewaert, D. Delincé, R. Van Impe. Failure mechanisms and residual capacity of annealed glass/SGP laminated beams at room temperature. Engineering Failure Analysis 16 (2009) 1866–1875, https://doi.org/10.1016/j.engfailanal.2008.09.023
18. C. Bedon, J. Belis, A. Luible. Assessment of existing analytical models for the lateral torsional buckling analysis of PVB and SG laminated glass beams via viscoelastic simulations

and experiments. Engineering Structures 60 (2014) 52–67. https://doi.org/10.1016/j.engstruct.2013.12.012

19. R. Rafiee, A. Ghorbanhosseini. Developing a micro-macromechanical approach for evaluating long-term creep in composite cylinders. Thin–Walled Structures 151 (2020) 106714. https://doi.org/10.1016/j.tws.2020.106714
20. R. Rafiee, A. Ghorbanhosseini. Analyzing the long-term creep behavior of composite pipes: Developing an alternative scenario of short-term multi-stage loading test. Composite Structures 254 (2020) 112868. https://doi.org/10.1016/j.compstruct.2020.112868
21. R. Rafiee, B. Mazhari. Simulation of the long-term hydrostatic tests on Glass Fiber Reinforced Plastic pipes. Composite Structures 136 (2016) 56-63. https://doi.org/10.1016/j.compstruct.2015.09.058
22. R. Rafiee, B. Mazhari. Evaluating long-term performance of Glass Fiber Reinforced Plastic pipes subjected to internal pressure. Construction and Building Materials 122 (2016) 694–701. http://dx.doi.org/10.1016/j.conbuildmat.2016.06.103
23. R. Rafiee, B. Mazhari. Modeling creep in polymeric composites: Developing a general integrated procedure. International JournalofMechanicalSciences99(2015)112–120. http://dx.doi.org/10.1016/j.ijmecsci.2015.05.011
24. R.S. Lakes (1998) Viscoelastic Solids. Madison, Wisconsin: CRC Press.
25. L. Valarinho, J.R. Correia, M. Garrido, M. Sá, F.A. Branco. Flexural creep behavior of full-scale laminated glass panels. Journal of Structural Engineering 143 (2017) 04017139. https://doi.org/10.1061/(ASCE)ST.1943-541X.0001841
26. L. Galuppi, G. Royer-Carfagni. The post-breakage response of laminated heat-treated glass under in plane and out of plane loading. Composites Part B 147 (2018) 227–239. https://doi.org/10.1016/j.compositesb.2018.04.005
27. C. Bedon, J. Belis, A. Luible. Assessment of existing analytical models for the lateral torsional buckling analysis of PVB and SG laminated glass beams via viscoelastic simulations and experiments. Engineering Structures 60 (2014) 52–67. https://doi.org/10.1016/j.engstruct.2013.12.012
28. J. Belis, J. Depauw, D. Callewaert, D. Delincé, R. Van Impe. Failure mechanisms and residual capacity of annealed glass/SGP laminated beams at room temperature. Engineering Failure Analysis 16 (2009) 1866–1875, https://doi.org/10.1016/j.engfailanal.2008.09.023
29. L. Biolzi, S. Cattaneo, M. Orlando, L.R. Piscitelli, P. Spinelli. Post-failure behavior of Laminated Glass Beams Using Different Interlayers. Composite Structures 202 (2018) 578-589. https://doi.org/10.1016/j.compstruct.2018.03.009
30. P. Foraboschi. Analytical Solution of Two-Layer Beam Taking into Account Nonlinear Interlayer Slip. Journal of Engineering Mechanics 135 (2009) 1129-1146. https://doi.org/10.1061/(ASCE)EM.1943-7889.0000043

31. A. Patenaude. Technics Topics: Distortion in Sealed Glazing Units. Progressive Architecture 72 (2012) 43-45
32. Draft prEN 16613:2013 Glass in Building - Laminated Glass and Laminated Safety Glass - Determination of Interlayer Mechanical Properties
33. M. Martín, X. Centelles, A. Solé, C. Barreneche, A.I. Fernández, L.F. Cabeza. Polymeric interlayer materials for laminated glass: A review. Construction and Building Materials 230 (2020) 116897. https://doi.org/10.1016/j.conbuildmat.2019.116897
34. L. Biolzi, S. Cattaneo, G. Rosati. Progressive damage and fracture of laminated glass beams. Construction and Building Materials 24 (2010) 577–584. https://doi.org/10.1016/j.conbuildmat.2009.09.007
35. C. Louter, J. Belis, F. Veer, J.-P. Lebet. Durability of SG-laminated reinforced glass beams: Effects of temperature, thermal cycling, humidity and load-duration. Construction and Building Materials 27 (2012) 280–292. https://doi.org/10.1016/j.conbuildmat.2011.07.046
36. K. Martens, R. Caspeele, J. Belis. Experimental investigations of statically indeterminate reinforced glass beams. Construction and Building Materials 119 (2016) 296–307. https://doi.org/10.1016/j.conbuildmat.2016.04.151
37. C. Bedon, M. Santarsiero. Laminated glass beams with thick embedded connections – Numerical analysis of full-scale specimens during cracking regime. Composite Structures 195 (2018) 308-324. https://doi.org/10.1016/j.compstruct.2018.04.083
38. M. Santarsiero, C. Bedon, C. Louter. Experimental and numerical analysis of thick embedded laminated glass connections. Composite Structures 188 (2018) 242-256. https://doi.org/10.1016/j.compstruct.2018.01.002
39. EN 1991-1-1:2009. Eurocode 1: Actions on structures – Part 1-1: General actions – Densities, self-weight, imposed loads for buildings (2009) Brussels.
40. M. Fröling and K. Persson, Computational methods for laminated glass. Journal of Engineering Mechanics, (2013) 780-79 https://doi.org/10.1061/(ASCE)EM.1943-7889.0000527
41. Kuraray Europe GmbH. Trosifol Architectural Laminated Glass Interlayers, Germany, 2018, p.9.
42. W.D. Callister Jr., D.G. Rethwisch. Materials Science and Engineering: An Introduction. vol. 1. 8th ed. 2009. https://doi.org/10.1017/CBO9781107415324.004
43. M. López-Aenlle, F. Pelayo, G. Ismael, M.A. García Prieto, A. Martín Rodríguez, A. Fernández-Canteli. Buckling of laminated-glass beams using the effective-thickness concept. Composite Structures 137 (2016) 44–55. http://dx.doi.org/10.1016/j.compstruct.2015.11.014
44. Muniz-Calvente M, Ramos A, Fernández P, Lamela MJ, Álvarez A, Fernández-Canteli A. Probabilistic failure analysis for real glass components under general loading conditions. Fatigue Fract Eng Mater Struct. 2019;42:1283–1291. https://doi.org/10.1111/ffe.13011

45. M. Gergesova, B. Zupančič, I. Saprunov, I. Emri. The closed form t-T-P shifting (CFS) algorithm. Journal of Rheology 55 (2011) 1-16. https://doi.org/10.1122/1.3503529

Data availability

The raw data required to reproduce these findings are available upon request.